Journal of Neuroimmunology 331 (2019) 74–86

Contents lists available at ScienceDirect

Journal of Neuroimmunology

journal homepage: www.elsevier.com/locate/jneuroim

Microglia are continuously activated in the circumventricular organs of mouse brain

Shohei Takagi[a], Eriko Furube[a], Yousuke Nakano[a,b], Mitsuhiro Morita[c], Seiji Miyata[a,*]

[a] Department of Applied Biology, Kyoto Institute of Technology, Matsugasaki, Sakyo-ku, Kyoto 606-8585, Japan
[b] Department of Anatomy and Brain Science, Kansai Medical University, Hirakata, Japan
[c] Department of Biology, Graduate School of Science, Kobe University, Kobe, Japan

ARTICLE INFO

Keywords:
Microglia
Brain
CD16/32
CD86
CD206
Ym1
Amoeboid

ABSTRACT

Microglia are the primary resident immune cells of the brain parenchyma and transform into the amoeboid form in the “activated state” under pathological conditions from the ramified form in the “resting state” under physiologically healthy conditions. In the present study, we found that microglia in the circumventricular organs (CVOs) of adult mice displayed the amoeboid form with fewer branched cellular processes even under normal conditions; however, those in other brain regions showed the ramified form, which is characterized by well-branched and dendritic cellular processes. Moreover, microglia in the CVOs showed the strong protein expression of the M1 markers CD16/32 and CD86 and M2 markers CD206 and Ym1 without any pathological stimulation. Thus, the present results indicate that microglia in the CVOs of adult mice are morphologically and functionally activated under normal conditions, possibly due to the specialized features of the CVOs, namely, the entry of blood-derived molecules into parenchyma through fenestrated capillaries and the presence of neural stem cells.

1. Introduction

Microglia are resident macrophages in the brain, are diffusely distributed throughout the brain parenchyma, and function in immune defenses in the brain. These cells respond to many types of homeostatic disturbances in the brain and transform rapidly from the ramified form, so-called ‘resting microglia’, to the amoeboid form, referred to as ‘activated microglia’, under pathological brain conditions (Brown and Neher, 2014; Hanisch and Kettenmann, 2007). The transition from the resting to activated state has been attributed to a change in the functional phenotype rather than the awakening of cells because resting microglia actively survey the brain environment (Hanisch and Kettenmann, 2007; Nimmerjahn et al., 2005). Activated microglia participate in a number of functions such as phagocytosis and cytokine release (Kettenmann et al., 2011). In addition to morphological alterations, microglia rapidly up-regulate the expression of a large number of receptors and various secretory molecules that exert beneficial or harmful effects on damaged and inflamed brains (Hanisch and Kettenmann, 2007).

Peripheral macrophages have been shown to exhibit at least two distinct activation patterns (Colton, 2009; Cherry et al., 2014; Wang et al., 2014; Franco and Fernández-Suárez, 2015). The first activated state, the M1 phenotype, is typified as a classical proinflammatory response by the production of inflammatory cytokines and reactive oxygen species, antigen presentation, and the removal of pathogens. Macrophages may recognize harmful environmental stimuli and respond by producing proinflammatory cytokines including tumor necrosis factor α, interleukin-6, interleukin-1β, interferon-γ, and several chemokines (Boche et al., 2013; Cherry et al., 2014). Cytokine production is essential for the polarization of macrophages into the M1 phenotype (Mills et al., 2000). The expression of M1 marker proteins, such as low affinity IgG Fcγ receptor II/III (CD16/32), CD86, and major histocompatibility complex II (MHCII), is up-regulated to allow for antigen presentation and crosstalk with other cells (Taylor et al., 2005). M1 macrophages have the ability to produce reactive nitrogen species using nitric oxide synthase, which inactivates ion channels, damages

Abbreviations: BBB, blood-brain barrier; CD16/32, low affinity IgG Fcγ receptor II/III; CD206, mannose receptor C type 1; GFP, green fluorescent protein; PBS, phosphate-buffered saline; PBST, PBS containing 0.3% Triton X-100; TLR4, Toll-like receptor 4; Ym1, chitinase-like 3; CVOs, circumventricular organs; OVLT, organum vasculosum of the lamina terminalis; SFO, subfornical organ; ME, median eminence; AP, area postrema; MnPO, median preoptic nucleus; MPA, medial preoptic area; POA, preoptic area; vhc, ventral hippocampal commissure; fi, fimbria; Cx, cerebral cortex; Arc, arcuate hypothalamic nucleus; VMH, ventromedial hypothalamic nucleus; DG, dentate gyrus; Sol, nucleus of the solitary tract; 12 N, hypoglossal nucleus; 10 N, dorsal motor nucleus of the vagus

* Corresponding author.
E-mail address: smiyata@kit.ac.jp (S. Miyata).

http://dx.doi.org/10.1016/j.jneuroim.2017.10.008
Received 26 August 2017; Received in revised form 13 October 2017; Accepted 13 October 2017

DNA, and nitrates tyrosine residues that potentially inactivate enzymes and signal transduction (Bagasra et al., 1995; Murphy, 2000).

Another phenotype of activated macrophages is M2, which expresses mediators or receptors to down-regulate, repair, or protect the body from inflammation (Mantovani et al., 2004). M2 macrophages more strongly express mannose receptor C type 1 (CD206), chitinase-like 3 (Ym1), and arginase 1. Arginase 1 outcompetes the inducible function of nitric oxide synthase by attenuating the production of nitric oxide (Mantovani et al., 2004; Cherry et al., 2014). However, recent studies proposed that the M1/M2 categories have some limitations for their application to microglia (Martinez and Gordon, 2014; Randsohoff, 2016). The M1/M2 definitions are derived from data obtained when isolated macrophages were exposed to a simple stimulation in vitro. Furthermore, microglia in diseased brains often express the M1 and M2 marker proteins, and the states of microglia may not be isolated based on the M1 or M2 phenotype. In addition, the implication of the M1/M2 hypothesis is that macrophages clonally proliferate to maintain the M1 or M2 phenotype; however, there is currently no evidence to support this.

Previous studies demonstrated that microglia comprise diverse phenotypes rather than a uniform cell population in a manner that depends on brain regions under physiologically healthy conditions (Hanisch and Kettenmann, 2007; Gertig and Hanisch, 2014). Microglia display the region-dependent diversity of protein expression among brain regions (de Haas et al., 2008; Grabert et al., 2016). Microglia in the subventricular zone (SVZ) of adult mice are maintained in the activated state based on their semi-amoeboid morphology and stronger expression of CD45 and CD11b (Goings et al., 2006). Microglia in the SVZ exhibit stronger proliferative activity than those in other brain regions both in vivo (Goings et al., 2006) and in vitro (Marshall et al., 2008). Moreover, cultured microglia isolated from the SVZ have a higher proliferative capability and more sustained neurogenic niche than those in non-neurogenic brain regions (Marshall et al., 2014). Hippocampal and cerebellar microglia have higher ATP-producing capacity through the TCA cycle and the electron transport chain than other microglia in the brain (Grabert et al., 2016). Collectively, these findings indicate that the global gene expression profiles and functions of adult microglia in the healthy normal brain are regionally heterogeneous.

The adult brain vasculature generally has a blood-brain barrier (BBB) that prevents the free entry of water-soluble molecules into the brain parenchyma (Daneman and Barres, 2005; Daneman et al., 2010). Brain regions located around the third and fourth ventricles are named the circumventricular organs (CVOs) (Hofer, 1958) and are referred to as the “windows of the brain” (Gross and Weindl, 1987) (Fig. 1) because the vasculature of the CVOs lacks the BBB and allows the entry of blood-derived molecules or secretion of brain-synthesizing neuropeptides (Miyata and Morita, 2011; Mannari et al., 2013; Morita and Miyata, 2012; Mannari et al., 2016; Miyata, 2015, 2017). The CVOs comprise the organum vasculosum of the lamina terminalis (OVLT), subfornical organ (SFO), median eminence (ME), and area postrema (AP) (Sisó et al., 2010; Mimee et al., 2013; Miyata, 2015). The CVOs are important brain regions for the initiation of neuroinflammatory responses in the brain because circulating LPS and/or cytokines induce the faster transcriptional activation of genes that encode a wide number of proinflammatory molecules in the CVOs (Quan et al., 1997; Rummel et al., 2005; Yoshida et al., 2016). Moreover, the CVOs show dynamic structural reconstruction such as neurogenesis and gliogenesis (Hourai and Miyata, 2013; Furube et al., 2015) as well as angiogenesis (Morita et al., 2013, 2015; Furube et al., 2014). The CVOs have been suggested to play roles in many pathological conditions in humans such as sepsis, stress, the neuroinvasion of parasites, autoimmune encephalitis, and systemic amyloidosis (Sisó et al., 2010, 2012; Kristensson et al., 2013) because they are critically involved in most autonomic and endocrine regulatory pathways and lack the BBB.

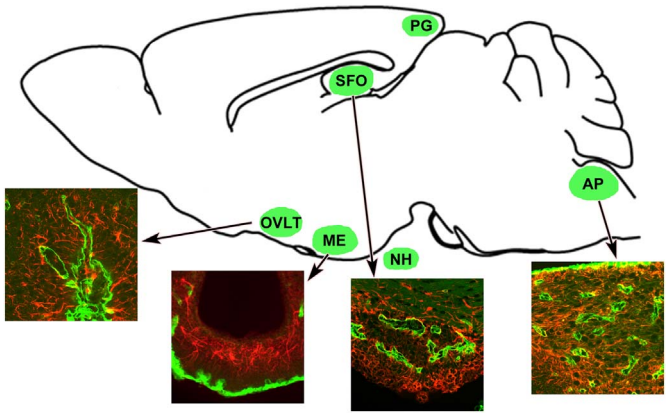

Fig. 1. Schematic illustration showing the location of the CVOs in the adult rodent brain. Insets indicate that the CVOs are characterized by dense and thick capillaries (green) and surrounding dense astrocyte networks (red). (For interpretation of the references to colour in this figure legend, the reader is referred to the web version of this article.)

Although microglia are presumed to participate in the reconstruction of cellular components by gliogenesis, neurogenesis, and angiogenesis as well as the removal of blood-derived molecules in the CVOs based on their functions, microglia in the CVOs have not yet been characterized. Therefore, we herein aimed to elucidate whether microglia in the CVOs of adult mice are continuously activated without any pathological stimulation. Microglia in the CVOs displayed the activated amoeboid form, even under physiologically healthy conditions. Moreover, microglia in the CVOs expressed high levels of the M1 markers CD16/32 and CD86 and M2 markers CD206 and Ym1. It is important to note that microglia expressing M1 and M2 marker proteins often localized in close contact with the vasculature and neural stem cells (NSCs)/progenitor cells (PCs). Thus, the present results indicate that microglia in the CVOs of adult mice are continuously maintained in their activated state under physiologically healthy conditions.

2. Materials and methods

2.1. Animals

Adult male mice (C57BL/6J) aged 8–12 weeks were used in the present experiments. In some experiments, we used *Nestin-CreERT2/CAG-CAT$^{loxP/loxP}$-EGFP* mice. *Nestin-CreERT2* mice (Okada et al., 2006) were crossed with *CAGCAT$^{loxP/loxP}$*-EGFP mice (Kawamoto et al., 2000) to obtain *Nestin-CreERT2/CAG-CAT$^{loxP/loxP}$-EGFP* animals. *Nestin-CreERT2/CAG-CAT$^{loxP/loxP}$*-EGFP mice received the single intraperitoneal administration of tamoxifen (180 mg/kg; Toronto Research Chemicals, Ontario, Canada) and were fixed 14 days after the final administration of tamoxifen. Animals were housed two per cage in a colony room with a 12-h light/dark cycle and given ad libitum access to commercial chow and tap water. Animal care and experiments were performed in accordance with the Guidelines laid down by the NIH and the Guidelines for the Proper Conduct of Animal Experiments Science Council of Japan. The experimental protocol was approved by the Animal Ethics Experimental Committee of the Kyoto Institute of Technology.

2.2. Antibodies and reagents

The following primary antibodies were used in the present experiments: rat IgG against mouse CD11b (clone 5C6, BIO-RAD, dilution 1:10,000), mouse CD86 (clone GL1, BD Pharmingen; dilution 1:200), mouse CD16/32 (clone 2.4G2, BD Pharmingen; dilution 1:400), and recombinant mouse Ym1 (clone#281926, R & D Systems; dilution 1:800); rabbit IgG against synthetic peptides corresponding to the C terminus of ionized calcium-binding adaptor molecule 1 (Iba1: 019-19741, Wako Chemicals, Osaka, Japan; dilution 1:800), and green

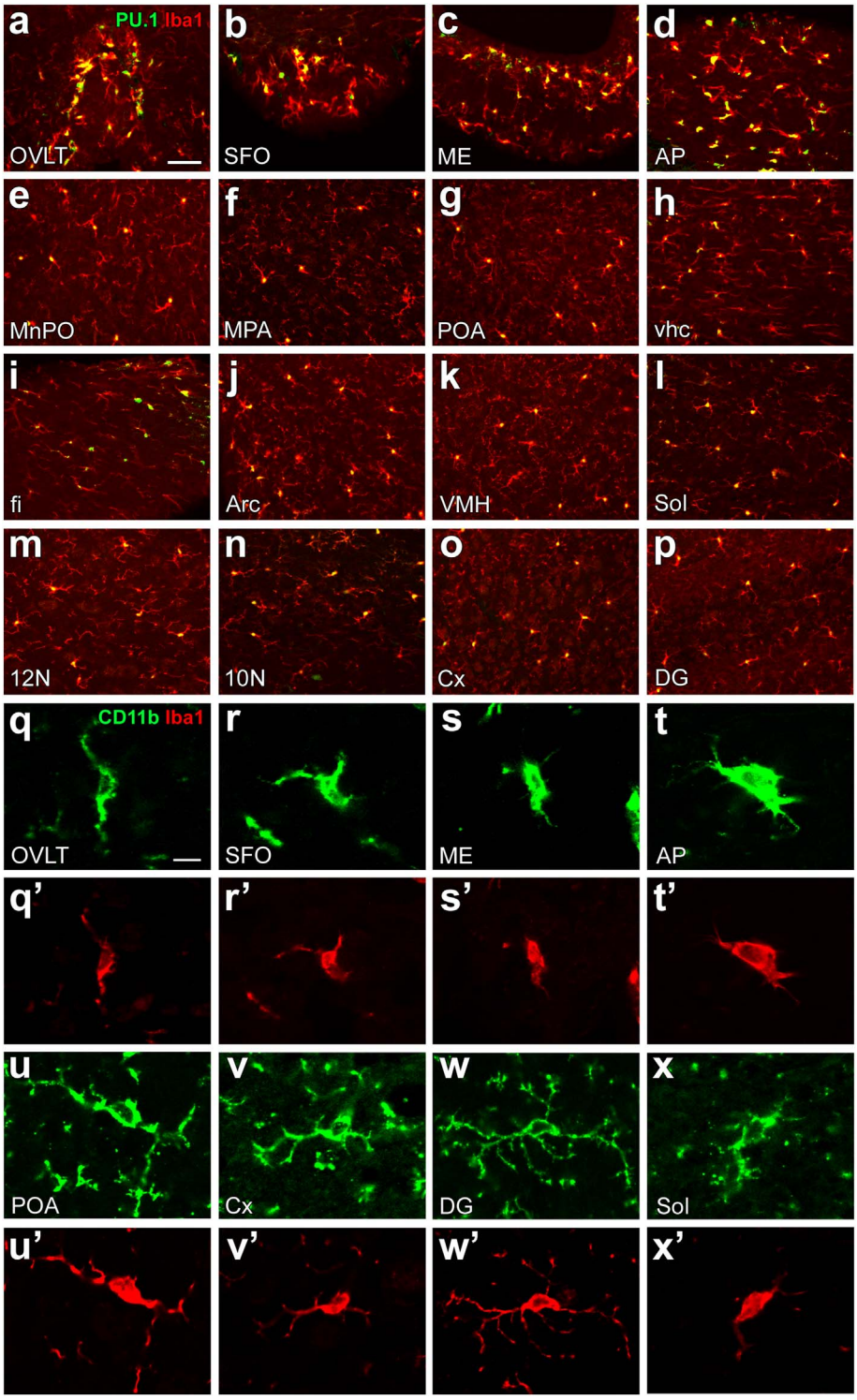

Fig. 2. Confocal images of PU.1, Iba1, and CD11b immunohistochemistries showing microglia/macrophages in the normal adult mouse brain. a–p; Double labeling immunohistochemistry revealed that PU.1$^+$ nuclei were unexceptionally observed at Iba1$^+$ microglia/macrophages in adult mouse brains. The density of PU.1$^+$ Iba1$^+$ microglia/macrophages was greater in the CVOs than in the other brain regions. q–x, q′–x′; Double labeling immunohistochemistry showed the colocalization of CD11b and Iba1. The immunoreactivity of CD11b was visible at the distal and core cellular processes of microglia, whereas that of Iba1 was mainly detected at core cellular processes. Scale bars = 50 (a) and 10 (q) μm.

fluorescent protein (GFP: A6455, Molecular Probes; dilution 1: 1000); mouse IgG amino acids 25–63 near the N terminus of mouse PU.1 (sc-390,405, Santa Cruz dilution 1:200); goat IgG against amino acids 19–1388 of recombinant CD206 (AF2535, R & D systems, dilution 1:400); guinea pig antibody against CX3CR1 (KIT−H27, dilution 1:800; Furube et al., 2017), and laminin (IM-2011, dilution 1:200; Imamura et al., 2010). In nuclear staining, sections were incubated with 4′,6-diamidino-2-phenylindole (DAPI; 1 μg/ml; Dojindo, Kumamoto, Japan).

2.3. Light microscopic immunohistochemistry

After deep anesthesia with urethane, mice were perfused transcardially with phosphate-buffered saline (PBS; pH 7.2) containing 0.1% trisodium citrate dihydrate followed by 4% paraformaldehyde (PFA) in 0.1 M phosphate buffer (PB, pH 7.4). After perfusion of the fixative, brains were dissected out, postfixed in 4% PFA in 0.1 M PB (pH 7.2) at 4 °C for 24 h, cryoprotected by 30% sucrose in PBS, and frozen quickly in Tissue-Tek OCT compound (Sakura Finetechnical, Tokyo, Japan). Sections were obtained by coronal slices on a cryostat (Leica, Wetzlar,

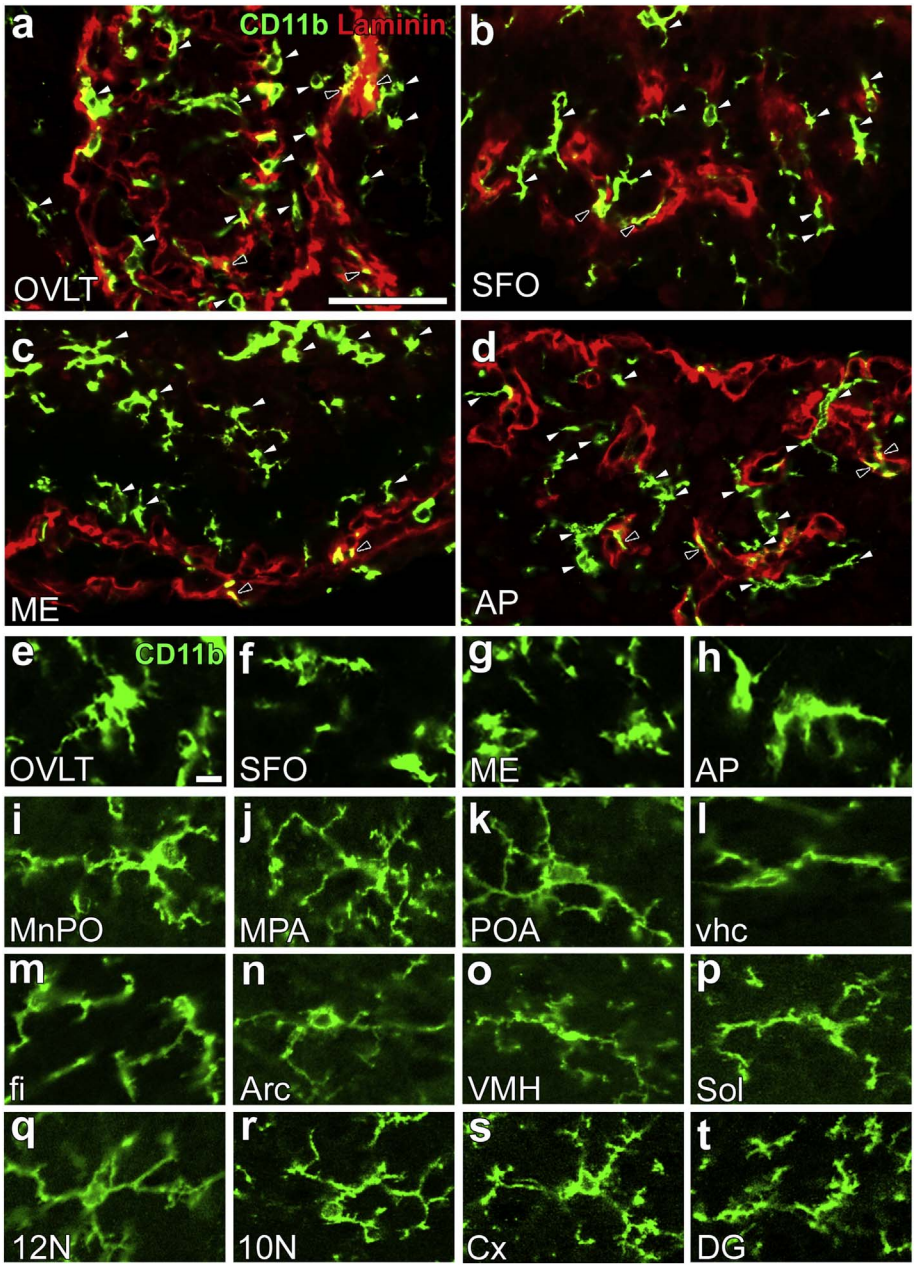

Fig. 3. Confocal images of CD11b immunohistochemistry revealing a unique microglial morphology in the CVOs of the normal adult mouse. a–d; Double labeling immunohistochemistry for CD11b and laminin distinguished microglia (open arrowheads) existing in the brain parenchyma from macrophages (solid arrowheads) in the laminin$^+$ perivascular space in the CVOs. e–t; The morphology of CD11b$^+$ microglia in the CVOs was the amoeboid type, which had less dendritic and shorter cellular processes. On the other hand, the morphology of CD11b$^+$ microglia in other brain regions was the ramified form, which had dendritic and long cellular processes. Scale bars = 50 (a) and 10 (e) μm.

Germany) at a thickness of 30 μm. In single and double labeling immunohistochemistry, a standard immunofluorescence technique was performed on free-floating sections according to our previous study (Hourai and Miyata, 2013). In brief, sections were washed with PBS and treated with 25 mM glycine in PBS for 20 min to quench remaining aldehyde residues. Sections were pretreated with 5% normal goat or horse serum in PBS containing 0.3% Triton X-100 (PBST) at 4 °C for 24 h to reduce the non-specific binding of IgG, and then incubated with the primary antibody at 4 °C for 48–72 h. They were then treated with Alexa488- or Alexa594-conjugated IgG (Jackson ImmunoResearch Laboratories, West Grove, PA; dilution 1:400) against rat, rabbit, goat, or guinea pig IgG in PBST containing normal serum for 2 h. In the case of the mouse primary antibody, sections were pretreated with an unlabeled goat Fab fragment against mouse IgG (Jackson ImmunoResearch; dilution 1:400) for 2 h to mask endogenous mouse IgG-like proteins, and Alexa488-conjugated goat F(ab)2 against mouse IgG was used (Jackson ImmunoResearch; dilution 1:100) to avoid the non-specific binding of endogenous mouse Fc receptors. The immunoreactivity of M1 and M2 proteins was not detected when the primary antibody was omitted.

Coverslips were sealed with Vectashield (Vector Labs, Burlingame, CA) and observations were performed using laser-scanning confocal microscopes (Fluoview, FV10i, OLYMPUS, Tokyo, Japan and TCS SP2 AOBS, Leica, Wetzlar, Germany). Images (1024 × 1024 pixels) were saved as TIF files by employing Olympus FV10-ASW Ver 1.7 Viewer or Leica Application Suite Advanced Fluorescence Lite 2.6.3 build 8173 and arranged using Photoshop 7.0.

2.4. Quantitative and statistical analyses

We analyzed at least 5 sections per animal in the OVLT and at least 8 sections per animal in the SFO, ME, AP, median preoptic nucleus (MnPO), medial preoptic area (MPA), preoptic area (POA), ventral hippocampal commissure (vhc), fimbria (fi), arcuate hypothalamic nucleus (Arc), ventromedial hypothalamic nucleus (VMH), nucleus of the solitary tract (Sol), hypoglossal nucleus (12 N), dorsal motor

nucleus of the vagus (10N), cerebral cortex (Cx), and dentate gyrus (DG). In the quantitative analysis, confocal images were obtained under the same pinhole size, brightness, and contrast setting. We saved images (1024 × 1024 pixels) as TIF files by employing Olympus FV10-ASW Ver 1.7 Viewer or Leica Application Suite Advanced Fluorescence Lite 2.6.3 build 8173 and arranged using Photoshop 7.0. Leica Application Suite Advanced Fluorescence Lite 2.6.3 build 8173 was used to generate the metric analysis of the total length of microglial processes and total number of microglial processes. The number of PU.1-labeled nuclei in Iba1-positive microglia and the area of CX3CR1-positive microglia, CD16/32-, CD86-, CD206-, and Ym-1-positive microglia/macrophages were measured using WinRoof, the threshold intensity of which was set to include measurement profiles by visual inspections and was kept constant. Data were expressed as the mean ± SEM. The significance of differences was assessed using a significance level of $P < 0.05$ by ANOVA with Tukey's post hoc test.

3. Results

3.1. Amoeboid-type microglia in the CVOs

In order to examine the density and morphology of microglia, we used the microglial/macrophage marker proteins PU.1, Iba1, and CD11b. Double labeling immunohistochemistry for PU.1 and Iba1 showed that PU.1$^+$ nuclei were exclusively present at Iba1$^+$ microglia/macrophages (Fig. 2a–p). The density of Iba1$^+$ microglia/macrophages containing PU.1$^+$ nuclei was greater in the CVOs (Fig. 2a–d) than in other brain regions (Fig. 2e–p). The co-expression of CD11b and Iba1 was observed at microglia in the OVLT (Fig. 2q, q′), SFO (Fig. 2r, r′), ME (Fig. 2s, s′), AP (Fig. 2t, t′), and other brain regions (Fig. 2u–x and u′–x′). The CD11b antibody employed had the ability to visualize the fine cellular processes of microglia, whereas only thick and core cellular processes were labeled with the Iba1 antibody. Collectively, these results indicate that the CD11b antibody is more useful for visualizing the fine morphology of microglia than Iba1, whereas the PU.1 and Iba1 antibodies were superior in terms of counting the number of microglia.

Double labeling immunohistochemistry for CD11b and laminin distinguished CD11b$^+$ microglia and macrophages by their localization to parenchyma and the perivascular space, respectively (Fig. 3a–d). High magnification views showed that the morphology of CD11b$^+$ microglia in the CVOs was the amoeboid form, even under physiologically healthy conditions (Fig. 3e–h). The morphology of CD11b$^+$ microglia in other brain regions was the ramified form with well-branched and long cellular processes (Fig. 3i–t).

The quantitative analysis revealed significant differences in the densities of PU.1$^+$ and Iba1$^+$ microglia/macrophages and the morphology of CD11b$^+$ microglia between the CVOs and other brain regions (Fig. 4). The density (number/mm^2) of microglia/macrophages was significantly higher in the CVOs (OVLT, 857.4 ± 77.9; SFO, 894.5 ± 33.8; ME, 1098.5 ± 28.3; AP, 1204.0 ± 39.8) than in other brain regions, ranging between 300.2 in the 12 N and 628.0 in the fimbria (Fig. 4a, Supplementary Table 1). The total length (μm) of microglial cellular processes was lower in the CVOs (OVLT, 65.8 ± 4.5; SFO, 65.5 ± 6.0; ME, 58.2 ± 2.2; AP, 63.5 ± 6.7) than in other brain regions (Fig. 4b, Supplementary Table 2). The total number of microglial cellular processes was lower in the CVOs (OVLT, 6.5 ± 0.5; SFO, 6.9 ± 0.3; ME, 6.7 ± 04; AP, 5.4 ± 0.5) than in other brain regions, ranging between 8.1 in the 12 N and 12.6 in the DG (Fig. 4c, Supplementary Table 3).

3.2. Strong expression of M1 markers in microglia/macrophages of the CVOs

In order to clarify whether microglia in the CVOs are functionally activated, we examined the expression of M1 and M2 marker proteins in adult mouse brains (Orihuela et al., 2016). We used two M1 marker

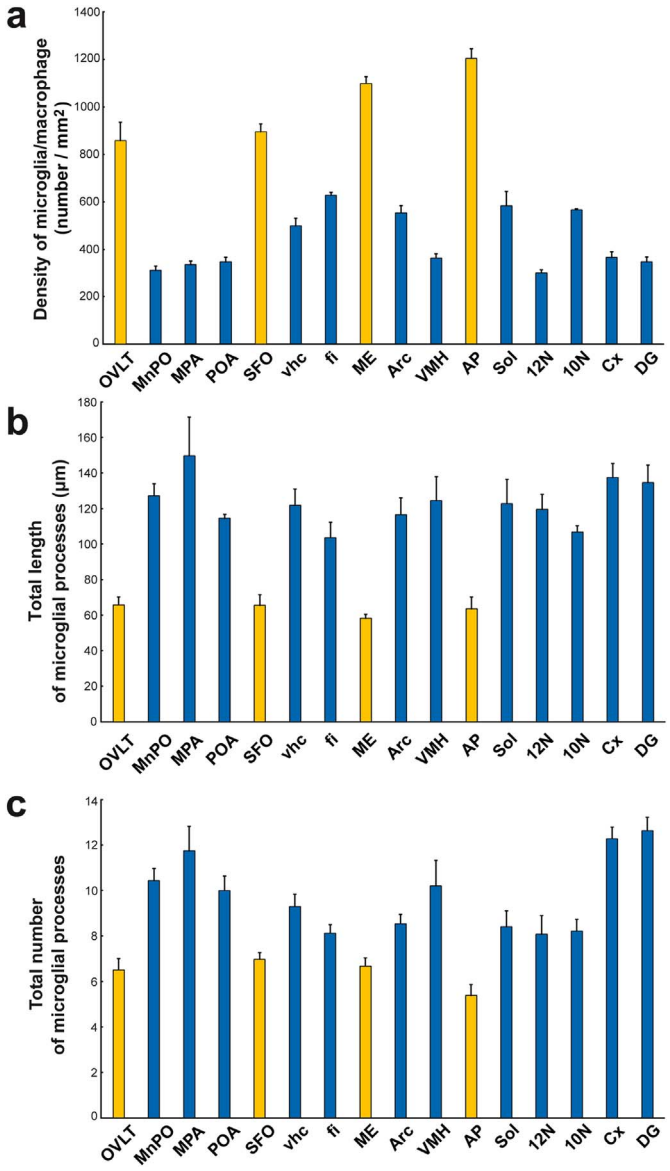

Fig. 4. A quantitative analysis showing brain region-dependent differences in the density of microglia/macrophages and morphology of microglia in normal adult mouse brains. a; The number of PU.1$^+$ and Iba1$^+$ microglia/macrophages was significantly larger in the CVOs than in other brain regions. b; The total length of the cellular processes of CD11b$^+$ microglia was shorter in the CVOs than in other brain regions. c; The total number of cellular processes of CD11b$^+$ microglia was shorter in the CVOs than in other brain regions. Data were expressed as the mean (± SE) of 4 animals. The statistical analysis by ANOVA with Tukey's post hoc test is shown in Supplementary Tables 1–3.

proteins; CD16/32 is concerned with phagocytosis and cytotoxicity, and CD86 is a type I membrane protein that belongs to the immunoglobulin superfamily and is responsible for antigen representation. The strong expression of CD16/32 was observed at microglia/macrophages in the CVOs (Fig. 5a–a″,c–c″, e–e″, g–g″) and the DG (Fig. 5i–i″), whereas it was weakly expressed in other brain regions (Supplementary Fig. 1). CD16/32$^+$ microglia often localized close to the laminin$^+$ vasculature in the OVLT, SFO, and AP, while this spatial association was not clearly observed in the ME or DG (Fig. 5b, d, f, h, j). CD16/32$^+$ macrophages were rarely detected in the laminin$^+$ perivascular space in the OVLT and ME, but were often observed in the SFO and AP. The quantitative analysis showed that the percentage of the CD16/32 − /CX3CR1-immunoreactive area was significantly higher in the OVLT, ME, and AP and may also be greater in the SFO and DG than in other brain regions (Fig. 5k, Supplementary Table 4). The percentage

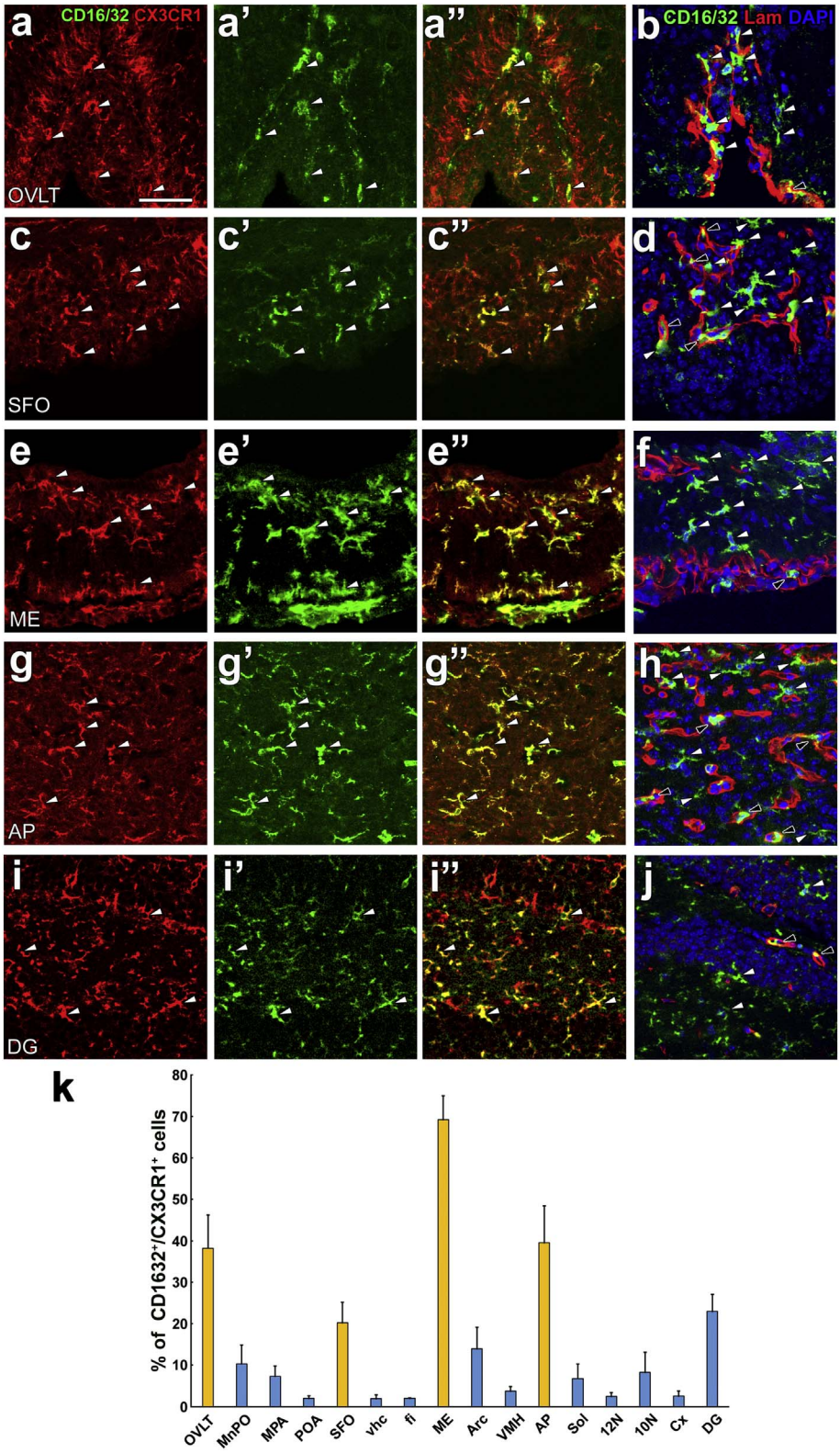

Fig. 5. Strong expression of the M1 marker, CD16/32, by microglia/macrophages in the CVOs and the DG of normal adult mouse brains. a–a″, c–c″, e–e″, g–g″, i–i″; A large number of CD16/32-immunoreactive CX3CR1$^+$ microglia/macrophages (open arrowheads) were noted in the CVOs and the DG. b, d, f, h, j; The expression of CD16/32 was observed at parenchymal microglia (open arrowheads) and perivascular macrophages (solid arrowheads) in the CVOs and the DG. Scale bar = 50 μm. k; The quantitative morphometric analysis showed that the percentage of the CD16/32-immunoreactive area in CX3CR1$^+$ microglia/macrophages was markedly higher in the CVOs than in other brain regions. Data were expressed as the mean (± SE) of 4 animals. The statistical analysis by ANOVA with Tukey's post hoc test is shown in Supplementary Table 4.

of the CD16/32-/CX3CR1-immunoreactive area was very high in the ME. The percentage of the CD16/32-immunoreactive microglial area in the total CD16/32-immunoreactive area was 62.3 ± 4.8 in the OVLT, 53.3 ± 5.2 in the SFO, 84.5 ± 1.1 in the ME, and 60.3 ± 4.8 in the AP.

Another M1 marker, CD86 was also frequently expressed in nearly 25% of microglia/macrophages in the CVOs (Fig. 6a–a″, c–c″, e–e″, g–g″), while it expression was negligible in other brain regions (Supplementary Fig. 2). A few CD86$^+$ microglia localized close to the laminin$^+$ vasculature in the OVLT, SFO, and AP, while this spatial association was not clearly observed in the ME (Fig. 6b, d, f, h). CD86$^+$ macrophages were also detected at the laminin$^+$ perivascular space in the CVOs. The quantitative analysis showed that the percentage of the CD86-/CX3CR1-immunoreactive area was significantly higher in the

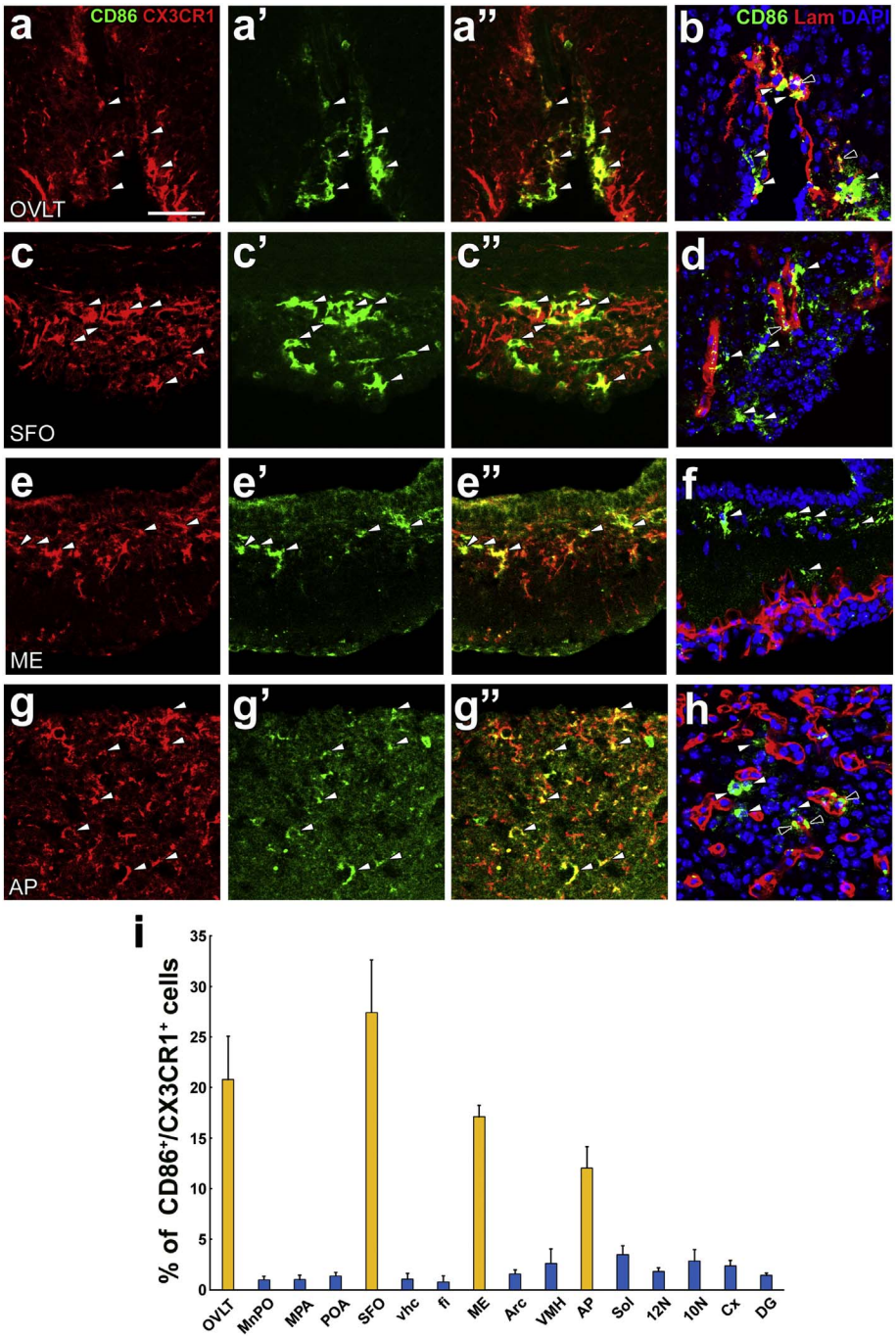

Fig. 6. Strong expression of the M1 marker, CD86, at microglia/macrophages in the CVOs of normal adult mouse brains. a–a″, c–c″, e–e″, g–g″; A large number of CD86-immunoreactive CX3CR1$^+$ microglia/macrophages (open arrowheads) were noted in the CVOs. b, d, f, h; The expression of CD86 was observed at parenchymal microglia (open arrowheads) and perivascular macrophages (solid arrowheads). Scale bar = 50 μm. i; The quantitative morphometric analysis showed that the percentage of the CD86-immunoreactive area in CX3CR1$^+$ microglial/macrophages was significantly larger in the CVOs than in other brain regions. Data were expressed as the mean (± SE) of 4 animals. The statistical analysis by ANOVA with Tukey's post hoc test is shown in Supplementary Table 5.

CVOs than in other brain regions (Fig. 6e, Supplementary Table 5). The percentage of the CD86-immunoreactive microglial area in the total CD86-immunoreactive area was 61.1 ± 8.2 in the OVLT, 70.0 ± 5.4 in the SFO, 57.7 ± 5.3 in the ME, and 55.1 ± 11.1 in the AP.

3.3. Strong expression of M2 markers in microglia/macrophages of the CVOs

We also used two M2 type proteins; CD206 mediates the endocytosis of glycoproteins and Ym1 exhibits binding activity to chitin or glucosamine, but lacks chitinolytic activity. Similar to the M1 marker, the strong expression of CD206 was observed in nearly 25% of microglia/macrophages in the CVOs (Fig. 7a–a″, c–c″, e–e″, g–g″), whereas its expression was negligible in other brain regions (Supplementary Fig. 3). CD206$^+$ macrophages were often observed at the laminin$^+$ perivascular space in the CVOs (Fig. 7b, d, f, h). CD206$^+$ microglia sometimes localized close to the laminin$^+$ vasculature in the CVOs. The quantitative analysis showed that the percentage of the CD206-/CX3CR1-immunoreactive area was significantly higher in the CVOs than in other brain regions (Fig. 7i, Supplementary Table 6). The percentage of the CD206-immunoreactive microglial area in the total CD206-immunoreactive area was 42.0 ± 3.3 in the OVLT, 19.2 ± 3.7 in the SFO, 28.3 ± 4.8 in the ME, and 33.4 ± 5.2 in the AP.

Another M2 marker, Ym1 was expressed by microglia/macrophages in the CVOs (Fig. 8a–a″, c–c″, e–e″, g–g″). However, Ym1$^+$ microglia/macrophages were also observed in the DG (Fig. 8i–i″) and brain regions neighboring the CVOs such as the vhc, Arc, Sol, and 10 N (Supplementary Fig. 4). The expression of Ym1 was weak in brain regions distant from the CVOs (Supplementary Fig. 5). Most Ym1$^+$ microglia localized close to the laminin$^+$ vasculature in the OVLT, SFO, and AP

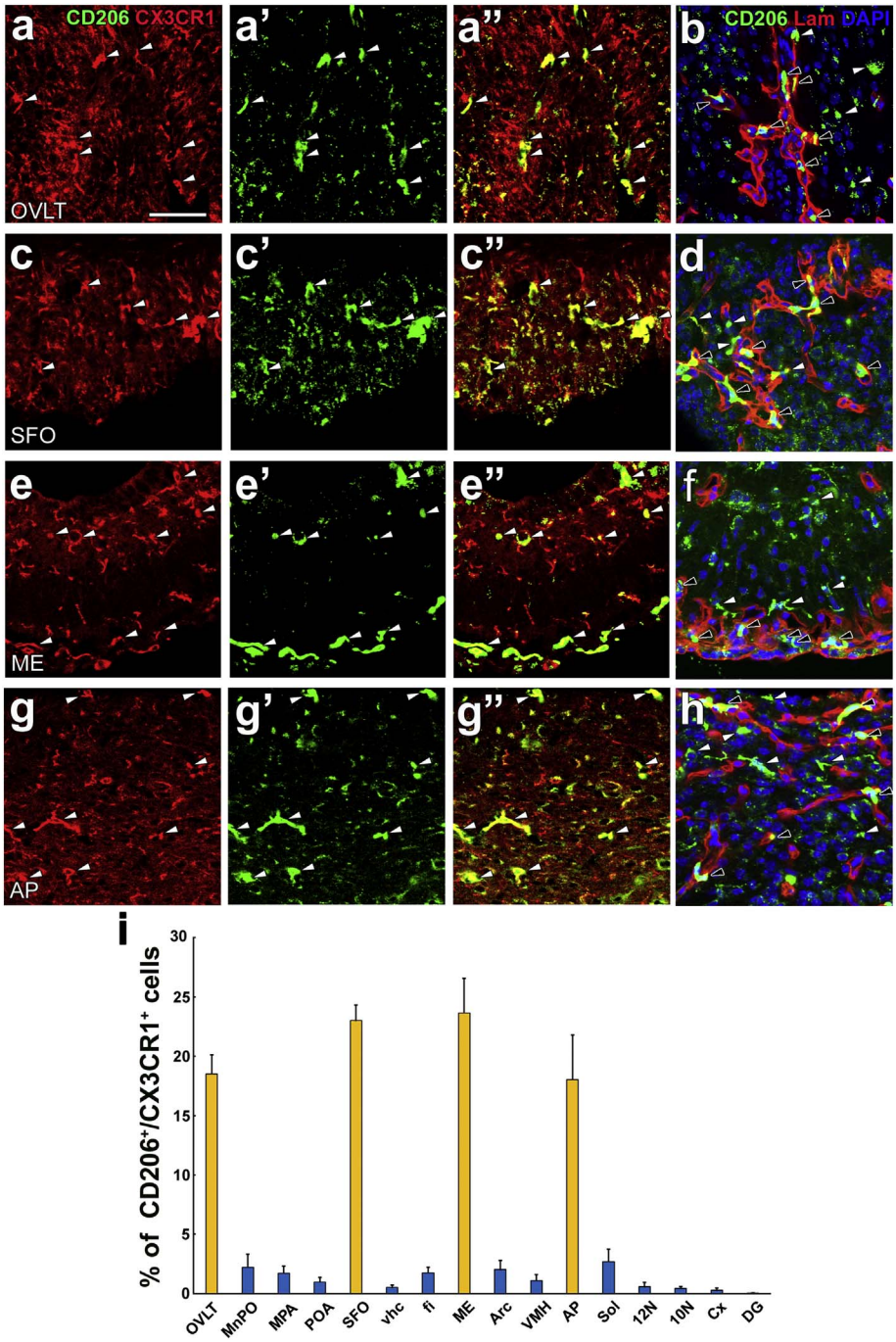

Fig. 7. Strong expression of the M2 marker, CD206, at microglia/macrophages in the CVOs of normal adult mouse brains. a–a″, c–c″, e–e″, g–g″; A large number of CD206-immunoreactive CX3CR1$^+$ microglia/macrophages (open arrowheads) were observed in the CVOs. b, d, f, h; The expression of CD206 was detected at parenchymal microglia (open arrowheads) and perivascular macrophages (solid arrowheads). Scale bar = 50 μm. i; The quantitative morphometric analysis showed that the percentage of the CD206-immunoreactive area in CX3CR1$^+$ microglia/macrophages was significantly larger in the CVOs than in other brain regions. Data were expressed as the mean (± SE) of 4 animals. The statistical analysis by ANOVA with Tukey's post hoc test is shown in Supplementary Table 6.

(Fig. 8b, d, h), whereas this spatial association was not observed in the ME or DG (Fig. 8f, j). Ym1$^+$ macrophages were rarely observed at the laminin$^+$ perivascular space in the CVOs and the DG. The quantitative analysis showed that the percentage of the Ym1-/CX3CR1-immunoreactive area was significantly higher in the OVLT and ME than in the other brain regions, being distant from the CVOs (Fig. 8k, Supplementary Table 7). The percentage of the Ym1-/CX3CR1-immunoreactive area was also higher in brain regions neighboring the CVOs such as the vhc, Arc, Sol, and 10 N. The percentage of the Ym1-immunoreactive microglial area in the total Ym1-immunoreactive area was 98.3 ± 1.3 in the OVLT, 90.4 ± 5.8 in the SFO, 95.2 ± 1.5 in the ME, and 91.5 ± 4.4 in the AP.

3.4. Spatial relationship between microglia and NSCs/PCs

We then examined the spatial association between microglia and NSCs/PCs. We used *Nestin-CreERT2/CAG-CAT$^{loxP/loxP}$-EGFP* to visualize NSCs and PCs. We found that CD11b$^+$ microglia were in close contact or engulfed GFP-expressing neural precursor cells/PCs (Fig. 9).

4. Discussion

The novel result of the present study is that microglia in the CVOs are maintained in their activated state, even under physiologically healthy conditions. This is supported by evidence showing that the morphology of microglia in the CVOs is the amoeboid form rather than the ramified form and also that the expression of M1 and M2 marker proteins is markedly stronger in the CVOs than in other brain regions.

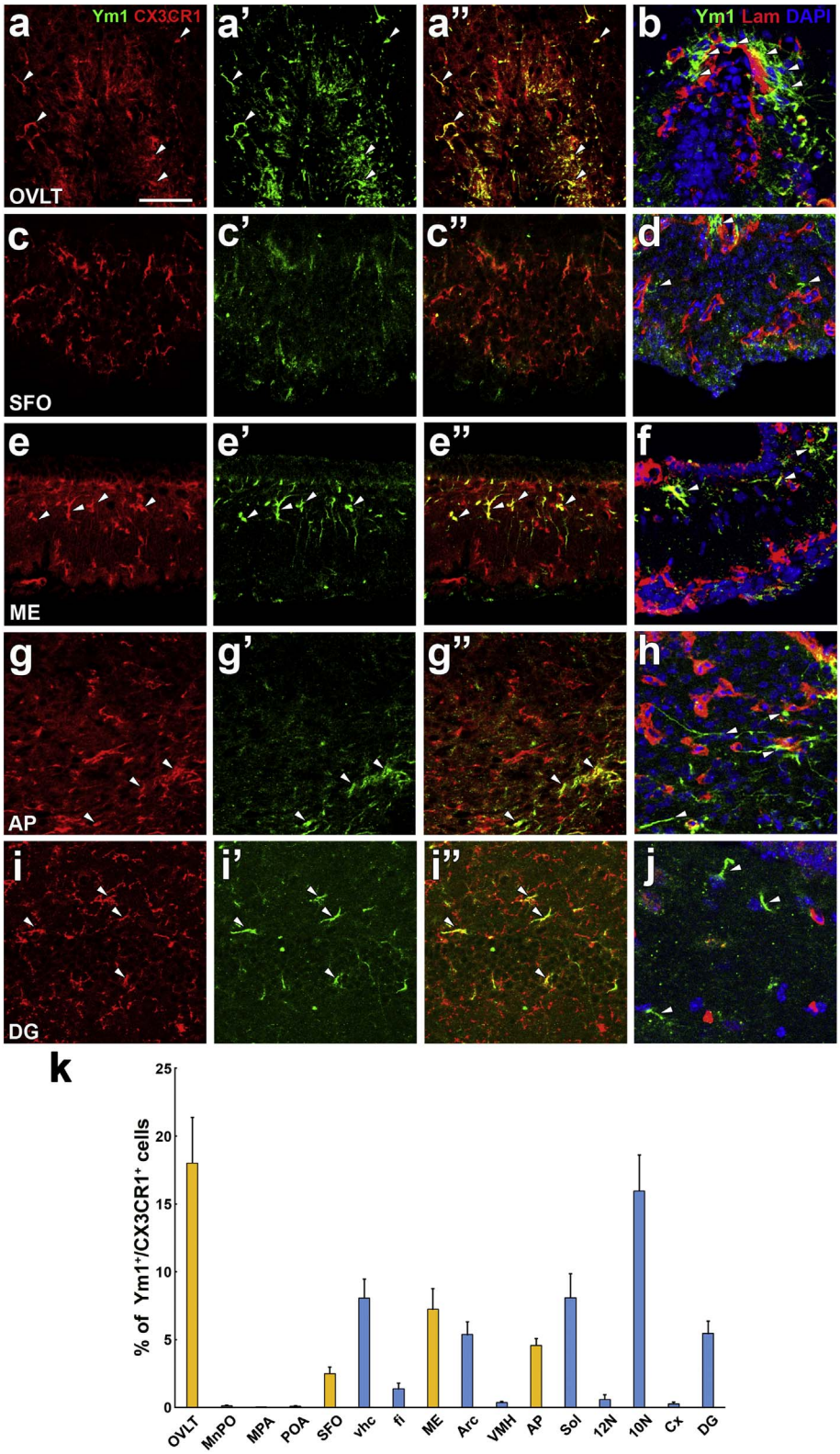

Fig. 8. Strong expression of the M2 marker, Ym1, at microglia/macrophages in the CVOs and the DG of normal adult mouse brains. a–a″, c–c″, e–e″, g–g″, i–i″; A large number of Ym1-immunoreactive CX3CR1$^+$ microglia/macrophages (open arrowheads) were observed in the CVOs and the DG. b, d, f, h, j; The expression of Ym1 was detected at parenchymal microglia (open arrowheads), but not at perivascular macrophages (solid arrowheads) in the CVOs and the DG. Scale bar = 50 μm. k; The quantitative morphometric analysis showed that the percentage of the Ym1-immunoreactive area in CX3CR1$^+$ microglia was higher in the CVOs and their neighboring brain regions. Data were expressed as the mean (± SE) of 4 animals. The statistical analysis by ANOVA with Tukey's post hoc test is shown in Supplementary Table 7.

The continuous activation of microglia in the CVOs may be responsible for tissue reorganization by NSCs/PCs and angiogenesis and/or the homeostasis of microenvironments in an attempt to protect the parenchyma from blood-derived toxic molecules.

The present results showed that the total length and number of microglial cellular processes was significantly smaller in the CVOs than in other brain regions, indicating that the microglial morphology of the CVOs is the amoeboid type. Microglia ramify and extend their cellular processes and continuously survey their microenvironment for potential threats under physiologically healthy conditions by moving their thin, highly branched processes, and have the ability to change into the activated amoeboid morphology in response to pathophysiological brain insults (Gordon, 2003; Ransohoff and Perry, 2009; Brown and Neher, 2014; Hanisch and Kettenmann, 2007). Activated microglia

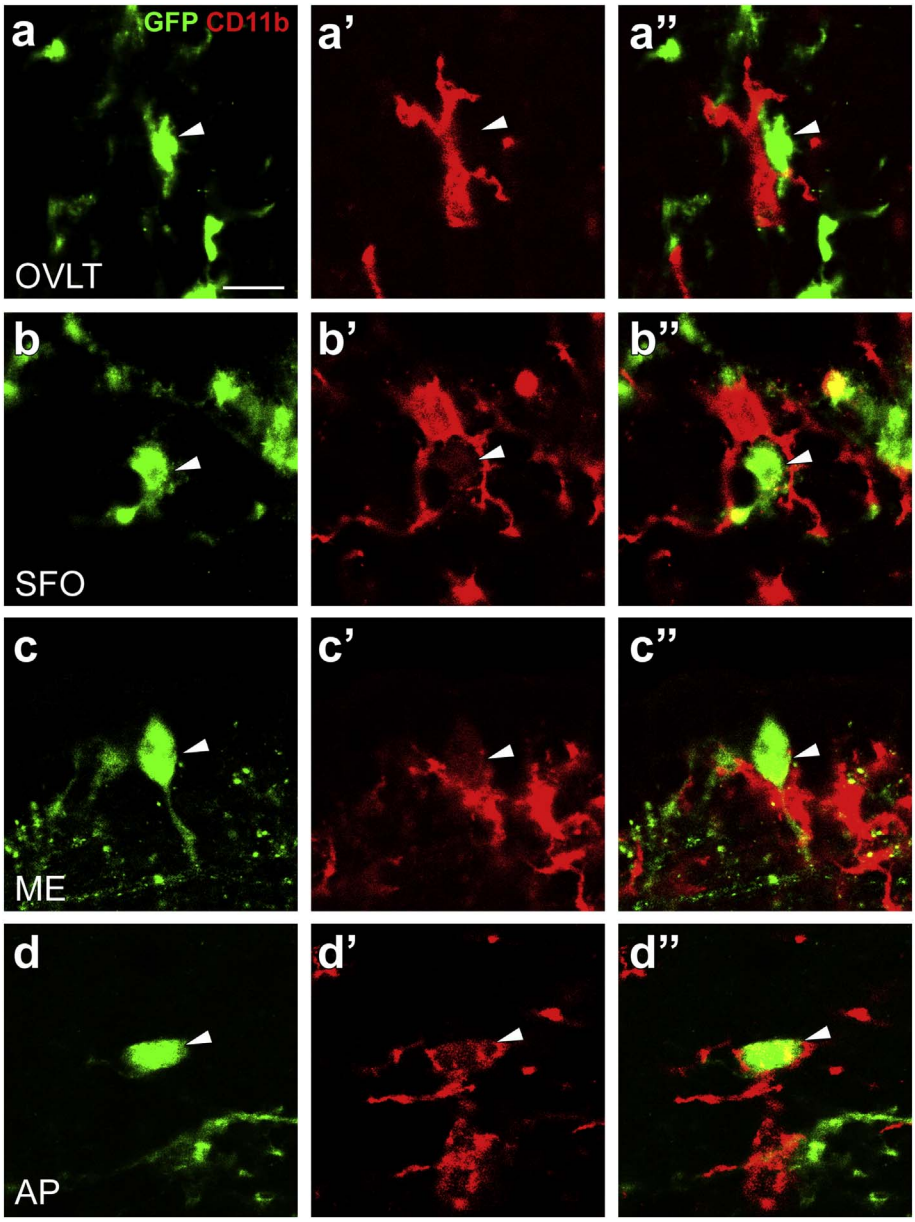

Fig. 9. Spatial association between microglia and neural stem/progenitor cells in the CVOs of normal brains of Nestin-CreERT2/CAG-CAT$^{loxP/loxP}$-EGFP mice. CD11b^{+} microglia were in close contact with EGFP-expressing NSPCs (arrowheads). Scale bar = 10 μm.

assume their amoeboid morphology with the decreased motility of cellular processes upon pathological stimuli (Orr et al., 2009). Changes in the microglial morphology correspond to an increase in phagocytotic activity and/or inflammatory cytokine production (Perry et al., 2010; Morrison and Filosa, 2013). In addition to the amoeboid morphology, the present study revealed that microglia in the CVOs expressed high levels of the activated microglia markers, M1 and M2 proteins; the expression of these marker proteins was prominent in diseased brains, but negligible in non-diseased brains. The expression of the M1 markers, CD16/32 and CD86 and M2 markers, CD206 and Ym1 was markedly stronger in the CVOs than in other brain regions. Thus, microglia in the CVOs are continuously activated based on the amoeboid morphology and the strong expression of activated marker proteins, even though animals were healthy and kept under normal conditions.

The reasons why microglia in the CVOs are continuously activated currently remain unclear. In the present study, CD16/32, CD86, CD206, and Ym1-expressing microglia were often found to be in close contact with fenestrated capillaries. This result suggests that activated microglia are closely involved in the vascular permeability and/or dynamics of fenestrated capillaries. The CVOs lack the BBB or endothelial tight junctions and allow the entry of blood-derived molecules into the parenchyma as well as the secretion of brain-derived bioactive molecules into the circulation (Morita and Miyata, 2012, 2013; Morita et al., 2016). A previous study reported that a large amount of blood-derived IgG enters the parenchyma in the CVOs by crossing over fenestrated capillaries (Natah et al., 2005). CD16/32 is a Fc receptor that cross links with monomeric IgG and mediates phagocytosis against antibody-coated pathogens and soluble proteins (Swanson and Hoppe, 2004; Nimmerjahn and Ravetch, 2008). The recognition of antigens by MHCII and the stimulation of its co-stimulatory factor CD86 are responsible for antigen presentation and subsequent T cell proliferation, differentiation, and cytokine secretion (Medzhitov, 2001). CD206 on macrophages mediates the recognition and binding of the mannosylated carbohydrates of various pathogens, leading to the endocytosis of pathogens (Régnier-Vigouroux, 2003). Based on the functions of these M1 and M2 marker proteins and entry of blood-derived molecules, activated microglia may phagocytize neurotoxic blood-derived molecules or cells in order to maintain the parenchymal microenvironment in the CVOs.

Another possible functional role of activated microglia is their involvement in the structural dynamics of the CVOs. We recently

demonstrated the presence of continuous angiogenesis with the proliferation and apoptosis of endothelial cells in the CVOs (Morita et al., 2013, 2016; Furube et al., 2014). Conditioned medium obtained from resting microglia inhibited the proliferation of brain endothelial cells, while that from activated microglia promoted it (Welser et al., 2010). The activation of microglia has been shown to increase the density of vascular branching in the retina (Biswas et al., 2017). Microglia often localize in close contact with developing blood vessels and a lack of microglia reduces the numbers of vascular branches in the retina (Kubota et al., 2009; Rymo et al., 2011). Thus, activated microglia may control the proliferation of endothelial cells and/or removal of apoptotic endothelial cells.

In the CVOs, NSCs have been reported to mainly differentiate into oligodendrocyte PCs (Furube et al., 2015). In the present study, we found that microglia in *Nestin-CreERT2/CAG-CAT$^{loxP/loxP}$-EGFP* mice sometimes engulfed GFP-expressing NSCs/PCs. Neurogenesis and oligodendrogenesis are both blocked by endotoxin-activated microglia, but are induced by microglia activated by the cytokines interleukin-4 or interferon-γ, indicating that the microglial phenotype critically affects their ability to support renewal from adult NSCs/PCs (Butovsky et al., 2006). Activated microglia in the SVZ of developing brains significantly promote neurogenesis and oligodendrogenesis, together with the production of a number of proinflammatory cytokines (Shigemoto-Mogami et al., 2014). Microglia in the SVZ of the adult mouse brain have been reported to express phosphorylated signal transducer and activator of transcription 6, release a distinct set of cytokines, and play a crucial role in the survival and migration of neural PCs (NPCs) (Ribeiro Xavier et al., 2015). In a model of experimental autoimmune encephalomyelitis, NSCs were activated and initiated regeneration in order to supply new oligodendrocytes during acute disease, but lost this regenerating ability during chronic phases; however, the inhibition of microglia with a minocycline treatment improved the proliferation of NSCs and oligodendrocyte PCs originating in the SVZ as well as their differentiation into mature oligodendrocytes (Muzio et al., 2010; Rasmussen et al., 2011). Previous in vitro studies demonstrated that the differentiation of NPCs in the supernatant of M1 microglia resulted in neurogenesis, while exposure to M2 supernatants led to oligodendrogenesis (Butovsky et al., 2006; Yuan et al., 2017). In the present study, microglia in the DG expressed high levels of CD16/32 and Ym1; however, the morphology of the DG was in the ramified form. Ym1 is a novel mammalian lectin that exhibits pH-dependent, specific affinity towards glucosamine oligomers and heparin (Sun et al., 2001). Ym1 is also known to alert the immune system to damage via the interleukin-1-mediated activation of interleukin-17-producing T cells (Sutherland et al., 2014). Most newborn NPCs undergo apoptosis in the first one to four days after differentiation into NPCs and are cleared through phagocytosis by microglia in the DG (Sierra et al., 2010). Microglia also control the number of NPCs (Mosher et al., 2012; Cunningham et al., 2013; Nikolakopoulou et al., 2013). The close interaction between NSCs, PCs, and the vasculature indicates glial and NPC interactions in the perivascular niche (Goldman and Chen, 2011). The present result showing that M1 and M2 marker-expressing microglia were likely to closely localize with fenestrated capillaries supports this possibility. Thus, activated microglia may play a role in the control of oligodendrogenesis and neurogenesis by acting NSCs and/or their PCs.

In the present study, we also found that a large number of macrophages in the perivascular space expressed the M1 markers, C16/32 and CD86, and M2 marker, CD206, but did not express the M2 marker, Ym1. A previous study reported that CD163-expressing macrophages in the perivascular space sequestered dextran 10 kDa (molecular weight 10,000) in the AP within 5 min of the administration of the fluorescent tracer (Willis et al., 2007). Perivascular macrophages in the pineal gland, which has been classified as a CVO and lacks the BBB, express the M1 marker, MHCII and exhibit phagocytotic activity (Kaur et al., 1997; Møller et al., 2006). Virchow-Robin perivascular spaces surround the walls of arteries, arterioles, veins, and venules as they course from the subarachnoid space through the brain parenchyma (Robin, 1859). Macrophages in Virchow-Robin perivascular spaces express high levels of the M1 marker, MHCII, and exhibit strong phagocytotic activity (Bechmann and Nitsch, 1997; Bechmann et al., 2001a). Moreover, the rapid replacement of macrophages in Virchow-Robin perivascular spaces has been reported in adult mice using transplants of GFP-transfected bone marrow cells (Bechmann et al., 2001b). Peripheral macrophages may have dendritic cell-like functions because they leave perivascular spaces via the bloodstream in order to reach peripheral lymphatic organs (KoÈsel et al., 1997). Thus, macrophages in the perivascular spaces of the CVOs may exhibit phagocytotic and antigen-presenting activities.

Acknowledgments

This work was supported in part by Scientific Research Grants from the Japan Society for the Promotion of Science (No. 16K07027) and a Research Fellowship of the Japan Society for the Promotion of Science for Young Scientists (No. 16J10225). We are grateful to Drs. H. Okano, R. Kageyama, J. Miyazaki, and Francois Renault-Mihara for their generous supply of Nestin-CreERT2 and CAG-CATloxP/loxP-EGFP transgenic mice.

Appendix A. Supplementary data

Supplementary data to this article can be found online at https://doi.org/10.1016/j.jneuroim.2017.10.008.

References

Bagasra, O., Michaels, F.H., Zheng, Y.M., Bobroski, L.E., Spitsin, S.V., Fu, Z.F., Tawadros, R., Koprowski, H., 1995. Activation of the inducible form of nitric oxide synthase in the brains of patients with multiple sclerosis. Proc. Natl. Acad. Sci. U. S. A. 92, 12041–12045.

Bechmann, I., Nitsch, R., 1997. Astrocytes and microglial cells incorporate degenerating fibers following entorhinal lesion: a light, confocal, and electron microscopical study using a phagocytosis-dependent labeling technique. Glia 20, 145–154.

Bechmann, I., Priller, J., Kovac, A., Böntert, M., Wehner, T., Klett, F.F., Bohsung, J., Stuschke, M., Dirnagl, U., Nitsch, R., 2001a. Immune surveillance of mouse brain perivascular spaces by blood-borne macrophages. Eur. J. Neurosci. 14, 1651–1658.

Bechmann, I., Kwidzinski, E., Kovac, A.D., Simbürger, E., Horvath, T., Gimsa, U., Dirnagl, U., Priller, J., Nitsch, R., 2001b. Turnover of rat brain perivascular cells. Exp. Neurol. 168, 242–249.

Biswas, S., Bachay, G., Chu, J., Hunter, D.D., Brunken, W.J., 2017. Laminin-dependent interaction between astrocytes and microglia: a role in retinal angiogenesis. Am. J. Pathol.(17) pii: S0002-9440. (30417-0).

Boche, D., Perry, V.H., Nicoll, J.A., 2013. Review: activation patterns of microglia and their identification in the human brain. Neuropathol. Appl. Neurobiol. 39, 3–18.

Brown, G.C., Neher, J.J., 2014. Microglial phagocytosis of live neurons. Nat. Rev. Neurosci. 15, 209–216.

Butovsky, O., Ziv, Y., Schwartz, A., Landa, G., Talpalar, A.E., Pluchino, S., Martino, G., Schwartz, M., 2006. Microglia activated by IL-4 or IFN-gamma differentially induce neurogenesis and oligodendrogenesis from adult stem/progenitor cells. Mol. Cell. Neurosci. 31, 149–160.

Cherry, J.D., Olschowka, J.A., O'Banion, M.K., 2014. Neuroinflammation and M2 microglia: the good, the bad, and the inflamed. J. Neuroinflammation 11, 98.

Colton, C.A., 2009. Heterogeneity of microglial activation in the innate immune response in the brain. J. NeuroImmune Pharmacol. 4, 399–418.

Cunningham, C.L., Martínez-Cerdeño, V., Noctor, S.C., 2013. Microglia regulate the number of neural precursor cells in the developing cerebral cortex. J. Neurosci. 33, 4216–4233.

Daneman, R., Barres, B.A., 2005. The blood-brain barrier - lessons from moody flies. Cell 123, 9–12.

Daneman, R., Zhou, L., Kebede, A.A., Barres, B.A., 2010. Pericytes are required for blood-brain barrier integrity during embryogenesis. Nature 468, 562–566.

Marshall II, G.P., Deleyrolle, L.P., Reynolds, B.A., Steindler, D.A., Laywell, E.D., 2014. Microglia from neurogenic and non-neurogenic regions display differential proliferative potential and neuroblast support. Front. Cell. Neurosci. 8, 180.

Marshall II, G.P., Demir, M., Steindler, D.A., Laywell, E.D., 2008. Subventricular zone microglia possess a unique capacity for massive in vitro expansion. Glia 56, 1799–1808.

Franco, R., Fernández-Suárez, D., 2015. Alternatively activated microglia and macrophages in the central nervous system. Prog. Neurobiol. 131, 65–86.

Furube, E., Mannari, T., Morita, S., Nishikawa, K., Yoshida, A., Itoh, M., Miyata, S., 2014. VEGF-dependent and PDGF-dependent dynamic neurovascular reconstruction in the neurohypophysis of adult mice. J. Endocrinol. 222, 161–179.

Furube, E., Morita, M., Miyata, S., 2015. Characterization of neural stem cells and their progeny in the sensory circumventricular organs of adult mouse. Cell Tissue Res. 362, 347–365.
Furube, E., Kawai, S., Inagaki, H., Takagi, S., Morita, M., Miyata, S., 2017. Brain region-dependent heterogeneity and dose-dependent difference in transient microglia population increase during lipopolysaccharide-induced inflammation. Sci. Rep. 2017 (in press).
Gertig, U., Hanisch, U.K., 2014. Microglial diversity by responses and responders. Front. Cell. Neurosci. 8, 101.
Goings, G.E., Kozlowski, D.A., Szele, F.G., 2006. Differential activation of microglia in neurogenic versus non-neurogenic regions of the forebrain. Glia 54, 329–342.
Goldman, S.A., Chen, Z., 2011. Perivascular instruction of cell genesis and fate in the adult brain. Nat. Neurosci. 14, 1382–1389.
Gordon, S., 2003. Alternative activation of macrophages. Nat. Rev. Immunol. 3, 23–35.
Grabert, K., Michoel, T., Karavolos, M.H., Clohisey, S., Baillie, J.K., Stevens, M.P., Freeman, T.C., Summers, K.M., McColl, B.W., 2016. Microglial brain region-dependent diversity and selective regional sensitivities to aging. Nat. Neurosci. 19, 504–516.
Gross, P.M., Weindl, A., 1987. Peering through the windows of the brain. J. Cereb. Blood Flow Metab. 7, 662–671.
de Haas, A.H., Boddeke, H.W., Biber, K., 2008. Region-specific expression of immunoregulatory proteins on microglia in the healthy CNS. Glia 56, 888–894.
Hanisch, U.K., Kettenmann, H., 2007. Microglia: active sensor and versatile effector cells in the normal and pathologic brain. Nat. Neurosci. 10, 1387–1394.
Hofer, H., 1958. Zur morphologie der circumventrikulären ogane des zwischenhirns der säugetiere. Verhandl. Deut. Zool. Ges. 8, 202–251.
Hourai, A., Miyata, S., 2013. Neurogenesis in the circumventricular organs of adult mouse brains. J. Neurosci. Res. 91, 757–770.
Imamura, Y., Morita, S., Nakatani, Y., Okada, K., Ueshima, S., Matsuo, O., Miyata, S., 2010. Tissue plasminogen activator and plasminogen are critical for osmotic homeostasis by regulating vasopressin secretion. J. Neurosci. Res. 88, 1995–2006.
Kaur, C., Singh, J., Lim, M.K., Ng, B.L., Ling, E.A., 1997. Macrophages/microglia as 'sensors' of injury in the pineal gland of rats following a non-penetrative blast. Neurosci. Res. 27, 317–322.
Kawamoto, S., Niwa, H., Tashiro, F., Sano, S., Kondoh, G., Takeda, J., Tabayashi, K., Miyazaki, J., 2000. A novel reporter mouse strain that expresses enhanced green fluorescent protein upon Cre-mediated recombination. FEBS Lett. 470, 263–268.
Kettenmann, H., Hanisch, U.K., Noda, M., Verkhratsky, A., 2011. Physiology of microglia. Physiol. Rev. 91, 461–553.
KoÈsel, S., Egensperger, R., Bise, K., Arbogast, S., Mehraein, P., Graeber, M.B., 1997. Long-lasting perivascular accumulation of major histocompatibility complex class II-positive lipophages in the spinal cord of stroke patients: possible relevance for the immune privilege of the brain. Acta Neuropathol. 94, 532–538.
Kristensson, K., Masocha, W., Bentivoglio, M., 2013. Mechanisms of CNS invasion and damage by parasites. Handb. Clin. Neurol. 114, 11–22.
Kubota, Y., Takubo, K., Shimizu, T., Ohno, H., Kishi, K., Shibuya, M., Saya, H., Suda, T., 2009. M-CSF inhibition selectively targets pathological angiogenesis and lymphangiogenesis. J. Exp. Med. 206, 1089–1102.
Mannari, T., Morita, S., Furube, E., Tominaga, M., Miyata, S., 2013. Astrocytic TRPV1 ion channels detect blood-borne signals in the sensory circumventricular organs of adult mouse brains. Glia 61, 957–971.
Mantovani, A., Sica, A., Sozzani, S., Allavena, P., Vecchi, A., Locati, M., 2004. The chemokine system in diverse forms of macrophage activation and polarization. Trends Immunol. 25, 677–686.
Martinez, F.O., Gordon, S., 2014. The M1 and M2 paradigm of macrophage activation: time for reassessment. F1000Prime Rep. 6, 13.
Medzhitov, R., 2001. Toll-like receptors and innate immunity. Nat. Rev. Immunol. 1, 135–145.
Mills, C.D., Kincaid, K., Alt, J.M., Heilman, M.J., Hill, A.M., 2000. M-1/M-2 macrophages and the Th1/Th2 paradigm. J. Immunol. 164, 6166–6173.
Mimee, A., Smith, P.M., Ferguson, A.V., 2013. Circumventricular organs: targets for integration of circulating fluid and energy balance signals? Physiol. Behav. 121, 96–102.
Miyata, S., 2015. New aspects in fenestrated capillary and tissue dynamics in the sensory circumventricular organs of adult brains. Front. Neurosci. 9, 390.
Miyata, S., 2017. Advances in understanding of structural reorganization in the hypothalamic neurosecretory system. Front. Endocrinol (in press).
Miyata, S., Morita, S., 2011. A new method for visualization of endothelial cells and extravascular leakage in adult mouse brain using fluorescein isothiocyanate. J. Neurosci. Methods 202, 9–16.
Møller, M., Rath, M.F., Klein, D.C., 2006. The perivascular phagocyte of the mouse pineal gland: an antigen-presenting cell. Chronobiol. Int. 23, 393–401.
Morita, S., Miyata, S., 2012. Different vascular permeability between the sensory and secretory circumventricular organs of adult mouse brain. Cell Tissue Res. 349, 589–603.
Morita, S., Miyata, S., 2013. Accessibility of low-molecular-mass molecules to the median eminence and arcuate hypothalamic nucleus of adult mouse. Cell Biochem. Funct. 31, 668–677.
Morita, S., Ukai, S., Miyata, S., 2013. VEGF-dependent continuous angiogenesis in the median eminence of adult mice. Eur. J. Neurosci. 37, 508–518.
Morita, S., Furube, E., Mannari, T., Okuda, H., Tatsumi, K., Wanaka, A., Miyata, S., 2015. Vascular endothelial growth factor-dependent angiogenesis and dynamic vascular plasticity in the sensory circumventricular organs of adult mouse brain. Cell Tissue Res. 359, 865–884.
Morita, S., Furube, E., Mannari, T., Okuda, H., Tatsumi, K., Wanaka, A., Miyata, S., 2016. Heterogeneous vascular permeability and alternative diffusion barrier in sensory circumventricular organs of adult mouse brain. Cell Tissue Res. 363, 497–511.
Morrison, H.W., Filosa, J.A., 2013. A quantitative spatiotemporal analysis of microglia morphology during ischemic stroke and reperfusion. J. Neuroinflammation 10, 4.
Mosher, K.I., Andres, R.H., Fukuhara, T., Bieri, G., Hasegawa-Moriyama, M., He, Y., Guzman, R., Wyss-Coray, T., 2012. Neural progenitor cells regulate microglia functions and activity. Nat. Neurosci. 15, 1485–1487.
Murphy, M., 2000. Production of nitric oxide by glial cells: regulation and potential roles in the CNS. Glia 29, 1–13.
Muzio, L., Cavasinni, F., Marinaro, C., Bergamaschi, A., Bergami, A., Porcheri, C., Cerri, F., Dina, G., Quattrini, A., Comi, G., Furlan, R., Martino, G., 2010. Cxcl10 enhances blood cells migration in the sub-ventricular zone of mice affected by experimental autoimmune encephalomyelitis. Mol. Cell. Neurosci. 43, 268–280.
Natah, S.S., Mouihate, A., Pittman, Q.J., Sharkey, K.A., 2005. Disruption of the blood-brain barrier during TNBS colitis. Neurogastroenterol. Motil. 17, 433–446.
Nikolakopoulou, A.M., Dutta, R., Chen, Z., Miller, R.H., Trapp, B.D., 2013. Activated microglia enhance neurogenesis via trypsinogen secretion. Proc. Natl. Acad. Sci. U. S. A. 110, 8714–8719.
Nimmerjahn, F., Ravetch, J.V., 2008. Fcgamma receptors as regulators of immune responses. Nat. Rev. Immunol. 8, 34–47.
Nimmerjahn, A., Kirchhoff, F., Helmchen, F., 2005. Resting microglial cells are highly dynamic surveillants of brain parenchyma in vivo. Science 308, 1314–1318.
Okada, S., Nakamura, M., Katoh, H., Miyao, T., Shimazaki, T., Ishii, K., Yamane, J., Yoshimura, A., Iwamoto, Y., Toyama, Y., Okano, H., 2006. Conditional ablation of Stat3 or Socs3 discloses a dual role for reactive astrocytes after spinal cord injury. Nat. Med. 12, 829–834.
Orihuela, R., McPherson, C.A., Harry, G.J., 2016. Microglial M1/M2 polarization and metabolic states. Br. J. Pharmacol. 173, 649–665.
Orr, A.G., Orr, A.L., Li, X.J., Gross, R.E., Traynelis, S.F., 2009. Adenosine A(2A) receptor mediates microglial process retraction. Nat. Neurosci. 12, 872–878.
Perry, V.H., Nicoll, J.A., Holmes, C., 2010. Microglia in neurodegenerative disease. Nat. Rev. Neurol. 6, 193–201.
Quan, N., Whiteside, M., Kim, L., Herkenham, M., 1997. Induction of inhibitory factor kappaBalpha mRNA in the central nervous system after peripheral lipopolysaccharide administration: an in situ hybridization histochemistry study in the rat. Proc. Natl. Acad. Sci. U. S. A. 94, 10985–10990.
Randsohoff, R.M., 2016. A polarizing question: do M1 and M2 microglia exist? Nat. Neurosci. 19, 987–991.
Ransohoff, R.M., Perry, V.H., 2009. Microglial physiology: unique stimuli, specialized responses. Annu. Rev. Immunol. 27, 119–145.
Rasmussen, S., Imitola, J., Ayuso-Sacido, A., Wang, Y., Starossom, S.C., Kivisäkk, P., Zhu, B., Meyer, M., Bronson, R.T., Garcia-Verdugo, J.M., Khoury, S.J., 2011. Reversible neural stem cell niche dysfunction in a model of multiple sclerosis. Ann. Neurol. 69, 878–891.
Régnier-Vigouroux, A., 2003. The mannose receptor in the brain. Int. Rev. Cytol. 226, 321–342.
Ribeiro Xavier, A.L., Kress, B.T., Goldman, S.A., Lacerda de Menezes, J.R., Nedergaard, M.A., 2015. Distinct population of microglia supports adult neurogenesis in the subventricular zone. J. Neurosci. 35, 11848–11861.
Robin, T., 1859. Recherches sur quelques particulariteÂs de la structure des capillaires de leÁncephale. J. Appl. Physiol. 2, 537–719.
Rummel, C., Voss, T., Matsumura, K., Korte, S., Gerstberger, R., Roth, J., Hübschle, T., 2005. Nuclear STAT3 translocation in guinea pig and rat brain endothelium during systemic challenge with lipopolysaccharide and interleukin-6. J. Comp. Neurol. 491, 1–14.
Rymo, S.F., Gerhardt, H., Wolfhagen, S.F., Uv, A., Betsholz, C., 2011. A two-way communication between microglial cells and angiogenic sprouts regulates angiogenesis in aortic ring cultures. PLoS One 6, e15846.
Shigemoto-Mogami, Y., Hoshikawa, K., Goldman, J.E., Sekino, Y., Sato, K., 2014. Microglia enhance neurogenesis and oligodendrogenesis in the early postnatal subventricular zone. J. Neurosci. 34, 2231–2243.
Sierra, A., Encinas, J.M., Deudero, J.J., Chancey, J.H., Enikolopov, G., Overstreet-Wadiche, L.S., Tsirka, S.E., Maletic-Savatic, M., 2010. Microglia shape adult hippocampal neurogenesis through apoptosis-coupled phagocytosis. Cell Stem Cell 7, 483–495.
Sisó, S., Jeffrey, M., González, L., 2010. Sensory circumventricular organs in health and disease. Acta Neuropathol. 120, 689–705.
Sisó, S., Martin, S., Konold, T., Hawkins, S.A., Thurston, L., Simmons, M.M., Stack, M.J., Jeffrey, M., González, L., 2012. Minimal involvement of the circumventricular organs in the pathogenesis of spontaneously arising and experimentally induced classical bovine spongiform encephalopathy. J. Comp. Pathol. 147, 305–315.
Sun, Y.J., Chang, N.C., Hung, S.I., Chang, A.C., Chou, C.C., Hsiao, C.D., 2001. The crystal structure of a novel mammalian lectin, Ym1, suggests a saccharide binding site. J. Biol. Chem. 276, 17507–17514.
Sutherland, T.E., Logan, N., Rückerl, D., Humbles, A.A., Allan, S.M., Papayannopoulos, V., Stockinger, B., Maizels, R.M., Allen, J.E., 2014. Chitinase-like proteins promote IL-17-mediated neutrophilia in a tradeoff between nematode killing and host damage. Nat. Immunol. 15, 1116–1125.
Swanson, J.A., Hoppe, A.D., 2004. The coordination of signaling during Fc receptor-mediated phagocytosis. J. Leukoc. Biol. 76, 1093–1103.
Taylor, P.R., Martinez-Pomares, L., Stacey, M., Lin, H.H., Brown, G.D., Gordon, S., 2005. Macrophage receptors and immune recognition. Annu. Rev. Immunol. 23, 901–944.
Wang, N., Liang, H., Zen, K., 2014. Molecular mechanisms that influence the macrophage m1-m2 polarization balance. Front. Immunol. 5, 614.
Welser, J.V., Li, L., Milner, R., 2010. Microglial activation state exerts a biphasic influence on brain endothelial cell proliferation by regulating the balance of TNF and TGF-β1. J. Neuroinflammation 7, 89.

Willis, C.L., Garwood, C.J., Ray, D.E., 2007. A size selective vascular barrier in the rat area postrema formed by perivascular macrophages and the extracellular matrix. Neuroscience 150, 498–509.
Yoshida, A., Furube, E., Mannari, T., Takayama, Y., Kittaka, H., Tominaga, M., Miyata, S., 2016. TRPV1 is crucial for proinflammatory STAT3 signaling and thermoregulation-associated pathways in the brain during inflammation. Sci Rep 6, 26088.
Yuan, J., Ge, H., Liu, W., Zhu, H., Chen, Y., Zhang, X., Yang, Y., Yin, Y., Chen, W., Wu, W., Yang, Y., Lin, J., 2017. M2 microglia promotes neurogenesis and oligodendrogenesis from neural stem/progenitor cells via the PPARγ signaling pathway. Oncotarget 8, 19855–19865.